Chinese Chemical Letters 36 (2025) 110602

Contents lists available at ScienceDirect

Chinese Chemical Letters

journal homepage: www.elsevier.com/locate/cclet

Photocatalyzed oxidation of water on oxygen pretreated rutile $TiO_2(110)$

Zhiqiang Wang[a,1], Yajie Gao[b,d,1], Tianjun Wang[b], Wei Chen[b], Zefeng Ren[b], Xueming Yang[b,c], Chuanyao Zhou[b,d,*]

[a] School of Physics, Xidian University, Xi'an 710071, China
[b] State Key Laboratory of Molecular Reaction Dynamics, Dalian Institute of Chemical Physics, Chinese Academy of Sciences, Dalian 116023, China
[c] Department of Chemistry, Southern University of Science and Technology, Shenzhen 518055, China
[d] University of Chinese Academy of Sciences, Beijing 100049, China

ARTICLE INFO

Article history:
Received 22 July 2024
Revised 29 October 2024
Accepted 31 October 2024
Available online 3 November 2024

Keywords:
Photocatalyzed oxidation of water
TiO_2
Terminal hydroxyl anions
•OH radicals
Interfacial charge transfer

ABSTRACT

The oxygen evolution reaction (OER) is the bottleneck in the overall photocatalytic splitting of water. The active sites (terminal titanium or bridging oxygen) and active species (molecular or dissociative water) of the initial step of the photocatalyzed OER on the prototypical photocatalyst TiO_2, remain debatable. Herein, the photocatalytic chemistry of monolayer water on oxygen-pretreated $TiO_2(110)$ (*o*-$TiO_2(110)$) and reduced $TiO_2(110)$ (*r*-$TiO_2(110)$) surfaces initiated by 400 nm light illumination was investigated by time-dependent two-photon photoemission spectroscopy (TD-2PPE). The photoinduced reduction of the H_2O/*o*-$TiO_2(110)$ interface rather than the H_2O/*r*-$TiO_2(110)$ interface was detected by TD-2PPE. The difference in 2PPE originated from the presence of the terminal hydroxyl anions (OH_t^-) on H_2O/*o*-$TiO_2(110)$, as identified by X-ray photoelectron spectroscopy and temperature-programmed desorption. Therefore, the evolution of the electronic structure of H_2O/*o*-$TiO_2(110)$ was attributed to the photocatalyzed oxidation of the terminal hydroxyl anions, which most likely formed gaseous •OH radicals, reducing the interface. This work suggested that the oxidation of hydroxyl anions on top of the terminal titanium ions on TiO_2, which were excluded previously in solution, need to be considered in the mechanistic studies of the photocatalyzed OER.

Initiated by the seminal finding in 1972 [1], photocatalyzed water splitting into H_2 and O_2 has become the center of solar-to-chemical conversion because of the cleanness and high energy density of hydrogen fuel, which is expected to alleviate and eventually solve the energy and environmental problems [2,3]. Although various photocatalysts have been developed, TiO_2 is still widely used in both scientific and technological fields owing to its stability, low cost, nontoxicity and relatively high activity [2–9]. Therefore, it has become a prototype for studying the fundamental processes in photocatalysis.

The oxygen evolution reaction (OER) is the bottleneck in the overall photocatalytic splitting of water because of the involvement of multiple holes [10]. Despite its great significance, the molecular mechanism for the photocatalyzed OER in solution is still under intensive debate [11,12]. While the OER is suggested to be initiated by the photocatalyzed oxidation of bridging hydroxyls anions (Figs. 1A and B) into adsorbed •OH radicals through interfacial hole transfer [12], it is challenged by the mismatch between the highest occupied molecular orbital (HOMO) of the surface hydroxyl anions and the valence band maximum (VBM) of the TiO_2 substrate (Fig. 2).

A Lewis acid–base mechanism has then been proposed where nucleophilic attack of water on a trapped hole at the bridging oxygen sites takes place [11,13,14]. Both the interfacial charge transfer and Lewis acid–base mechanisms emphasize the importance of the bridging sites on TiO_2 in the photocatalyzed OER and indicate the minimal role of terminal Ti ions (fivefold coordinated Ti, Ti_{5c}) [11,12] which are preferential adsorption sites [15]. In addition, no consensus on the generation of free •OH radicals from irradiated TiO_2 suspensions has been reached [16–18].

Surface science studies, however, report the photocatalzyed oxidation of water at the Ti_{5c} sites of TiO_2 [19–22]. Although agreement regarding the reaction sites has been reached, the active species, *i.e.*, molecular or dissociative water at the terminal sites (H_2O_t or OH_t^-), are also debatable. In the theoretical field, Migani

* Corresponding author.
E-mail address: chuanyaozhou@dicp.ac.cn (C. Zhou).
[1] These authors contributed equally to this work.

https://doi.org/10.1016/j.cclet.2024.110602
1001-8417/

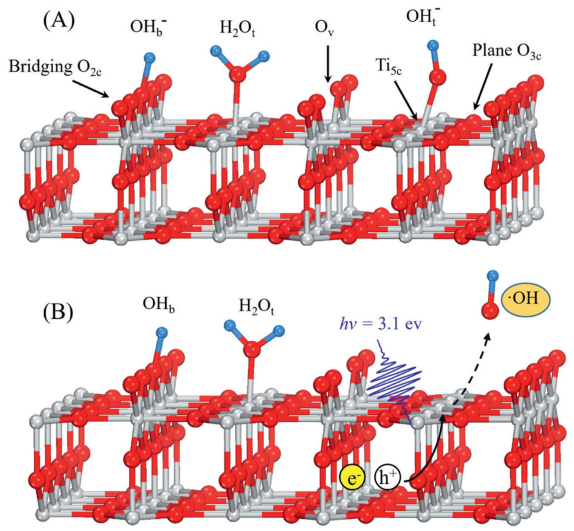

Fig. 1. (A) Structure of rutile TiO_2(110). The gray, red and blue spheres represent titanium, oxygen and hydrogen atoms, respectively. Terminal water (H_2O_t), terminal hydroxyl (OH_t^-) and bridging hydroxyl (OH_b^-) anions are indicated. Preferential adsorption sites, *i.e.*, the fivefold coordinated Ti (Ti_{5c}) and the bridging oxygen vacancy (O_v), are also shown. The bridging and terminal hydroxyl anions bind bidentately and monodentately, respectively, to the TiO_2 substrate. (B) Schematic illustration of the photocatalyzed oxidation of the terminal hydroxyl anions into gaseous ·OH radicals by holes. Bridging hydroxyl anions can also be photocatalytically oxidized to ·OH radicals. However, bidentate coordination may cause them difficult to desorb.

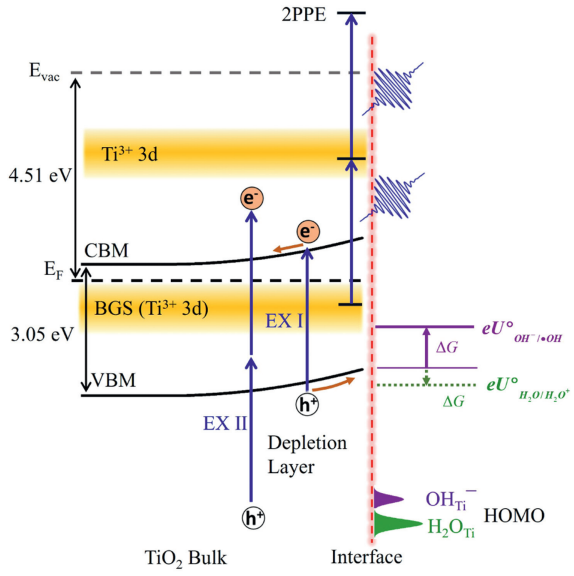

Fig. 2. Schematic illustration of the electronic structure at the H_2O/TiO_2(110) interface and two-photon photoemission from the band gap states (BGS). E_{vac}, E_F, CBM and VBM denote the vacuum level, the Fermi level, the conduction band minimum and the valence band maximum, respectively. The blue vertical arrow represents the absorption of one 400 nm photon. There are two band gap excitation pathways in this study: one-photon excitation (EX I) and two-photon excitation (EX II). The orange arrows show the direction of charge diffusion in the depletion layer. The olive- and violet-filled areas are the HOMOs of H_2O_t and OH_t^-, respectively. ΔG and U^o represent the redox free energy and the equivalent redox potential, respectively. ΔG is the energy difference between the initial and final states, *i.e.*, the reaction system with a completely free hole and a trapped hole, respectively. eU^o is the free energy level at which the hole is stabilized. The relative positions of the HOMO and eU^o are drawn according to references [16] and [13], respectively. Because of the unavailability at the solid-vacuum interface, the equivalent redox potentials are referred to as those at the solid–liquid interface. The filled golden area represents the split Ti^{3+} 3d orbitals, which contain the BGS and the empty states below and above the E_F, respectively. The absorption of one 400 nm photon excites the electrons in the BGS to the empty Ti^{3+} 3d orbitals (intra-atomic d-d transition), and the absorption of the second photon emits the excited electrons, giving rise to the 2PPE spectra.

et al. proposed that the oxidation of molecular water *via* a proton-coupled electron transfer process produced terminal ·OH radicals [23], but Wang *et al.* suggested that holes became involved only when water was converted into OH_t^- [24]. On the experimental side, using scanning tunneling microscopy (STM), Tan *et al.* concluded that water molecules at Ti_{5c} sites could be photocatalytically oxidized upon ultraviolet (UV) light illumination, producing neighboring bridging hydroxyl anions and gas phase ·OH radicals (Reaction 1) [19].

$$H_2O_t + O_b^{2-} + h^+ \rightarrow {}^{\bullet}OH_g + OH_b^- \quad (1)$$

where the subscripts t, b and g denote the adsorption at terminal Ti_{5c} sites and bridging oxygen sites and gas phase species, respectively, and h^+ represents a hole. In contrast, Xu *et al.* inferred that OH_t^- species were responsible for the oxidation reaction by considering the HOMO level of molecular and dissociative water relative to the VBM of TiO_2 [21]. In addition, the reported wavelength dependence of the photoactivity of water on TiO_2(110) varied from group to group. While Tan *et al.* suggested that H_2O_t on TiO_2(110) was active toward exposure to 400 nm, 355 nm, 266 nm and 193 nm light and that the oxidation efficiency was independent on the photon energy [19], Xu *et al.* showed that H_2O_t was inert until the illuminating light was below 290 nm and that the photoactivity increased with photon energy, suggesting that hot holes were needed to trigger the reaction [21].

Due to the existing controversies, the following questions need to be addressed: What are the active sites and the active species involved in the photocatalyzed oxidation of water on TiO_2(110)? And how does this reaction proceed? To answer these fundamental questions, the photocatalytic chemistry of the monolayer (ML; 1 ML = 5.2×10^{14} molecules/cm^2) water on oxygen-pretreated rutile TiO_2(110) (*o*-TiO_2(110)) and reduced TiO_2(110) (*r*-TiO_2(110)) triggered by 400 nm light illumination was investigated. Time-dependent two-photon photoemission spectroscopy (TD-2PPE) revealed the photoinduced reduction of the H_2O/*o*-TiO_2(110) interface; however, this phenomenon was not observed for H_2O/*r*-TiO_2(110). X-ray photoelectron spectroscopy (XPS) and temperature-programmed desorption (TPD) revealed the presence of the OH_t^- anions on H_2O/*o*-TiO_2(110) rather than on H_2O/*r*-TiO_2(110). By a thorough analysis, we propose that the photoinduced reduction of the H_2O/*o*-TiO_2(110) interface originates from the removal of OH_t^- anions on TiO_2 *via* photocatalyzed oxidation which likely produces gaseous ·OH radicals. This work suggests that Ti_{5c} ions in addition to bridging oxygen sites on TiO_2 and hydroxyl anions on top of them are active sites and active species in the photocatalyzed oxidation of water. Our results are highly beneficial to the study of the molecular mechanism of the generation of ·OH radicals and the photocatalyzed OER.

Adsorption state is the prerequisite to investigate the following surface chemistry. Thus, the adsorption of water on the *r*-TiO_2 and *o*-TiO_2 surfaces was first investigated by XPS and TPD (Fig. 3). For *r*-TiO_2(110), the Ti $2p_{3/2}$ spectrum was fitted using a main peak and a small shoulder centered at 459.5 eV and 457.3 eV (Fig. 3A); these are assigned to Ti^{4+} and Ti^{3+}, respectively [25]. The ratio between the peak areas of Ti^{3+} ($S_{Ti}{}^{3+}$) and Ti^{4+} ($S_{Ti}{}^{4+}$) was 3.4%, indicating a slight reduction of TiO_2(110). Upon annealing in oxygen, the binding energy of Ti^{4+} $2p_{3/2}$ decreased by 0.2 eV, and that of $S_{Ti}{}^{3+}/S_{Ti}{}^{4+}$ decreased substantially to 0.8% (Fig. 3B). Both the upward band bending and the decrease in the Ti^{3+} density were indicative of the oxidation of the substrate. The effect of the water adsorption on the Ti 2p XPS spectrum of both reduced and oxygen-pretreated TiO_2(110) was not evident (Figs. S1A and B in Supporting information). The O 1s XPS spectrum of clean *r*-TiO_2(110) showed a main peak at 530.8 eV and a shoulder at 532.2 eV (Fig. S1C in Supporting information); these peaks are attributed to lattice oxygen and bridging hydroxyls (from dissocia-

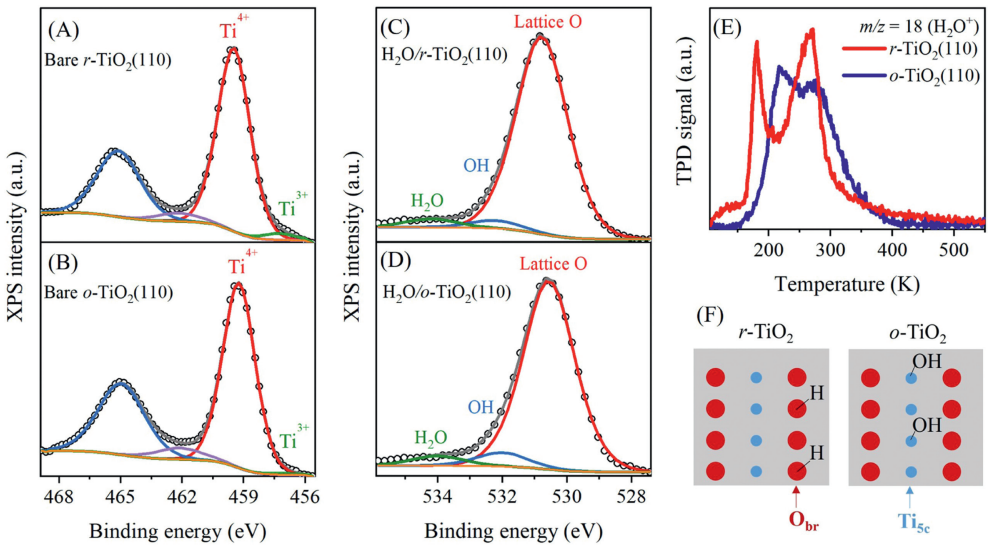

Fig. 3. Adsorption of water on *r*-TiO_2(110) and *o*-TiO_2(110). Ti 2p XPS spectra of the bare *r*-TiO_2(110) (A) and bare *o*-TiO_2(110) (B) showing the Ti^{3+} defects. O 1s XPS spectra of H_2O/*r*-TiO_2(110) (C) and H_2O/*o*-TiO_2(110) (D) showing the presence of the surface hydroxyl groups. All XPS spectra were acquired at a substrate temperature of 190 K. The XPS spectra were fitted by CasaXPS, and the center energy and peak area are shown in Tables S1 and S2 (Supporting information). (E) TPD spectra ($m/z = 18$) of water-covered *o*-TiO_2(110) and *r*-TiO_2(110). The water coverages in all XPS and TPD experiments are approximately 1.3 ML. (F) Illustration of the majority type of surface hydroxyls (bridging and terminal) on *r*-TiO_2(110) and *o*-TiO_2(110).

tion of residual water at oxygen vacancies (O_vs)), respectively [26]. After oxygen treatment, the center for the lattice and hydroxyl oxygen redshifted by 0.2 eV, consistent with that of Ti 2p. The ratios of the signal between hydroxyl (S_{OH}) and lattice oxygen (S_{OL}) after water adsorption were 4.0% and 7.2%, respectively, for *r*-TiO_2(110) and *o*-TiO_2(110).

TPD was used to measure the species on the water-covered TiO_2(110) surfaces (Fig. 3E). No desorption products other than water were detected. The TPD spectra of water from *r*-TiO_2 displayed two well-separated desorption features at 181 K and 266 K, and these were assigned to the bridging water (H_2O_b, bound to O_b through hydrogen bonding) and the terminal water, respectively [27]. The desorption of water between 400 K and 550 K indicated the recombination of the OH_b^-s [28]. Compared with water desorption from *r*-TiO_2, prominent changes in the desorption temperature and profile were observed for *o*-TiO_2: (1) The overall desorption temperature blue shift. The desorption of the second layer and the first layer shifted from 181 K to 218 K and from 266 K to 275 K, respectively. The second layer and first layer desorption peaks became much less resolved. (2) While the water desorption signals between 300 K and 400 K became substantially stronger, those in the region from 400 K to 550 K disappeared, which was consistent with the nearly vanishing Ti^{3+} defects in the XPS results. Moreover, these results were consistent with those from a previous TPD study [29].

The *o*-TiO_2 substrate was prepared by annealing the *r*-TiO_2(110) in an oxygen atmosphere (1×10^{-7} mbar) at 850 K followed by cooling in the same oxygen background until 475 K; afterward, the oxygen was evacuated. Annealing in oxygen at 850 K resulted in regular TiO_2(110)-(1 × 1) terraces with oxygen vacancies [29,30]. Further oxygen exposure at lower temperatures (from 850 K to 475 K in the present work) led to the titration of O_vs and the formation of terminal oxygen adatoms and TiO_x islands, generating an *o*-TiO_2(110) surface [30,31]. Water reacted with oxygen adatoms at Ti_{5c} sites to produce terminal hydroxyl anions [32,33]. The OH_t^- ions recombined as water and left the oxygen adatoms on TiO_2(110) between 300 K and 400 K [28,34]. In addition, water could be further stabilized on the roughened surface through hydrogen bonding [29,33]. These factors could contribute to the blueshift of the water desorption temperature on *o*-TiO_2(110). The inferior resolution between the TPD peaks from *o*-TiO_2(110) to *r*-TiO_2(110) could be ascribed to surface roughening upon oxygen treatment [29].

The adsorption states of water at the Ti_{5c} sites of TiO_2(110) are coverage dependent. Partial dissociation occurred below 0.4 ML, and molecular adsorption dominated above that point [35,36]. In this study, water at the Ti_{5c} sites of *r*-TiO_2(110) was in its molecular form when the coverage was approximately 1.3 ML. The surface hydroxyl species on H_2O/*r*-TiO_2(110), as detected by XPS, could be attributed to the OH_b^-s originating from the dissociation of water at the bridging O_vs. This assignment was further confirmed by the high-temperature (400–550 K) desorption of water in TPD. In contrast, no high-temperature water was detected on H_2O/*o*-TiO_2(110), indicating a negligible effect from the OH_b^- ions on this surface. The surface hydroxyls on *o*-TiO_2(110), which are present in XPS, could then be ascribed to the OH_t^-s. The OH_t^- ions recombined as water and desorbed at higher temperatures than terminal molecular water [28,34], in agreement with current TPD measurements. Therefore, the type of the hydroxyl groups on the water-covered *r*-TiO_2(110) and *o*-TiO_2(110) surfaces were predominantly bridging and terminal hydroxyl anions, respectively (Fig. 3F).

2PPE, which pumps electrons to excited states and then ionizes them by the absorption of two photons (Fig. 2), is a powerful tool to measure the electronic structure at surfaces and interfaces [37]. The evolution of the electronic structure of light irradiated H_2O/*o*-TiO_2 was monitored by TD-2PPE (Figs. 4A and B), while that of H_2O/*r*-TiO_2 is displayed in Fig. S2 (Supporting information) for comparison. In these experiments, the 400 nm femtosecond laser illuminated the H_2O/TiO_2 substrate continuously to trigger possible photochemical reactions and measured the electronic structure *via* 2PPE at the same time. The 2PPE spectra of bare *o*-TiO_2(110) are shown in Fig. 4C. The lower cutoff of the spectra, *i.e.*, the work function (WF) of bare *o*-TiO_2(110), is approximately 5.60 eV, and the signals of both *p*-polarized and *s*-polarized (not shown) light-excited 2PPE spectra, which are denoted as *p*-2PPE and *s*-2PPE, respectively, are very low. The high work function and weak 2PPE intensity indicate that only a few Ti^{3+}-related defects exist within the probe depth in the bare *o*-TiO_2 substrate [38]. The WF

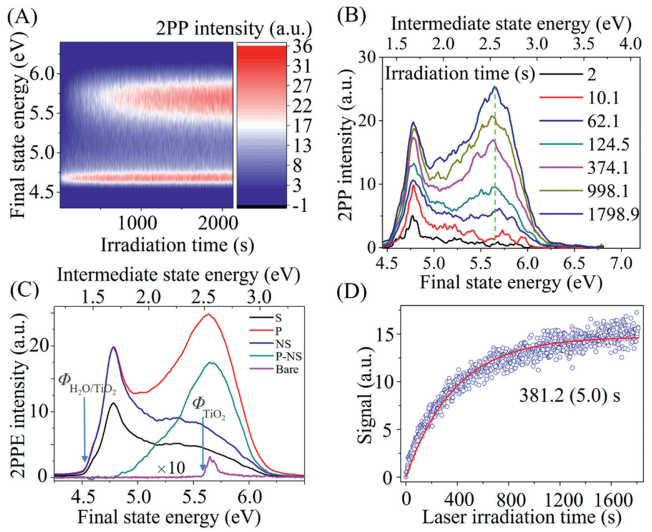

Fig. 4. (A) 2PPE spectra from the H_2O/*o*-TiO_2(110) interface as a function of illumination by *p*-polarized 400 nm probing light. (B) 2PPE spectra collected after the H_2O/*o*-TiO_2(110) interface was exposed to *p*-polarized 400 nm light for specified durations. (C) 2PPE spectra of bare and water covered *o*-TiO_2(110). For H_2O/*o*-TiO_2(110), the spectra were collected after 30 min of illumination. P and S represent the 2PPE spectra acquired with horizontally and vertically polarized light, respectively. P-NS represents the pure excited resonance signal that is obtained by subtracting the normalized S (NS) from P. (D) Integrated excited resonance signal (from 5.00 eV to 6.25 eV) as a function of irradiation time and a single exponential model fitting. The 2PPE spectra were collected at 120 K.

of bare *r*-TiO_2(110) is approximately 5.02 eV, and the 2PPE intensity (Fig. S2A) is approximately 67 times stronger than that of bare *o*-TiO_2(110).

Upon water adsorption, the WFs of *r*-TiO_2 and *o*-TiO_2 decrease to 4.37 and 4.52 eV, respectively, due to the formation of dipole layers [38]. While the *p*-2PPE spectrum of H_2O/*r*-TiO_2(110) shows a pronounced resonance at 2.55 eV, this feature is much less prominent in s-2PPE (Fig. S2A) and is consistent with the polarization dependence of 2PPE reported previously for H_2O/*r*-TiO_2 [39]. The 2PPE spectra from H_2O/*r*-TiO_2 were continuously collected and showed minimal changes (Fig. S2B). However, the evolution of the 2PPE spectra from the H_2O/*o*-TiO_2(110) interface was very different from that in a previous study where no resonance was detected [39]. A discussion regarding the origin of the difference is included in Supporting information. By continuously acquiring *p*-2PPE spectra of H_2O/*o*-TiO_2(110) immediately after the fresh interface was exposed to 400 nm probing light, changes in the electronic structure were captured and are shown in Figs. 4A and B. The resonance at 2.55 eV was absent initially, developed with light illumination and saturated after 30 min of irradiation; these results indicated a photoinduced change at the interface, which was in sharp contrast with that at the H_2O/*r*-TiO_2(110) interface. The integrated resonance signal (Fig. 4D) showed the evolution of the photoinduced changes at the H_2O/*o*-TiO_2(110) interface with a rising time constant of 381.2 s. The polarization dependence of the 2PPE spectra of the irradiated H_2O/*o*-TiO_2(110) (Fig. 4C) agreed with that of H_2O/*r*-TiO_2(110), indicating that the electronic structures of these two systems were of the same origin.

The schematic energetics of H_2O/TiO_2(110) are shown in Fig. 2. Because of the limited photon energy (3.10 eV), 2PPE is only able to detect electrons from band gap states (not from the valence band) whose density is proportional to the concentration of Ti^{3+} [40,41]. The intra-atomic d-d transition in Ti^{3+} of reduced TiO_2 led to the appearance of a resonance feature at 2.50 ± 0.20 eV in the 2PPE spectra [42,43]. This feature was absent at the beginning of the exposure of the fresh H_2O/*o*-TiO_2(110) interface to 400 nm light; this result indicated that *o*-TiO_2 had a very low Ti^{3+} density and was consistent with the XPS measurements. As the light illumination proceeded, the resonance signal became increasingly pronounced; thus, the density of Ti^{3+} at the H_2O/*o*-TiO_2(110) interface became increasingly higher, and the interface became increasingly reduced.

The reduction of TiO_2 is related to the creation of defects such as O_vs and Ti interstitials (Ti_{int}) [44,45], the desorption of electron acceptors [46] and the addition of electron donor atoms/molecules [41]. Photoinduced O_vs and/or Ti_{int}s generation on *o*-TiO_2(110) were ruled out because no 2PPE signal enhancement on bare *o*-TiO_2(110) was detected (Fig. S3 in Supporting information). This process on H_2O/*o*-TiO_2(110) was also unlikely since water could protect the TiO_2(110) surface from light-induced modification [47]. The inertness of the *o*-TiO_2(110) substrate suggested that the photoinduced change originated from the surface species. According to XPS and TPD measurements, H_2O_ts, H_2O_bs and OH_t^-s/OH_b^-s were present on the water covered *o*-TiO_2(110)/*r*-TiO_2(110) surfaces. The 2PPE spectra of H_2O/*r*-TiO_2(110) remained unchanged after prolonged light illumination, indicating that either the high coverage of H_2O and the OH_b^- ions on TiO_2(110) did not respond to 400 nm light or that their reaction-induced electronic structure change could not be detected by TD-2PPE.

Excluding H_2O_ts, H_2O_bs and OH_b^-s, the difference between the TD-2PPE results on H_2O/*o*-TiO_2(110) and H_2O/*r*-TiO_2(110) could only come from OH_t^-s. Terminal hydroxyls abstract excess electrons in the near-surface region of TiO_2(110) [28]. The reduction of OH_t^-/TiO_2(110) requires the deposition of electrons at the interface. Thermal processes, such as the reactions between H_2O_ts and OH_t^-s [48] and the recombination of OH_t^- pairs as water and oxygen adatoms [28,34], do not lead to net electron deposition/loss on TiO_2(110). In contrast, the oxidation of OH_t^- will leave electrons on the TiO_2(110) surface, causing the reduction of the substrate (Fig. 1B) according to Reaction 2. The desorption of hydroxyl radicals from UV-illuminated H_2O/TiO_2(110) was inferred in a previous STM study [19] and confirmed by time-of-flight mass spectrometry (TOF-MS) [20,21].

$$Ti^{4+} + OH_t^- + h^+ + e^- \rightarrow Ti^{3+} + {}^{\bullet}OH_g \quad (2)$$

Photocatalyzed production of gaseous $^{\bullet}$OH radicals from OH_t^-/TiO_2(110) can only occur at the wavelength lower than 300 nm [21]. According to theoretical calculations, near and supra band gap excitation of water covered TiO_2(110) produce adsorbed and free $^{\bullet}$OH radicals, respectively [23]. Another work also shows that the most stable structure of $^{\bullet}$OH radicals generated at Ti_{5c} sites by the transfer of thermalized holes is the adsorbed configuration [49]. In TD-2PPE, the 400 nm femtosecond laser triggers the changes at the H_2O/*o*-TiO_2(110) interface and probes the associated evolution of the electronic structure *via* two-photon photoemission. In addition to the near band gap excitation by absorbing one 400 nm photon (Excitation I in Fig. 2), another excitation pathway, *i.e.*, absorption of two 400 nm photons (Excitation II in Fig. 2), exists, because of the high peak power density of the femtosecond laser. This process can be justified by the two-photon photoemission from the band gap states of TiO_2, for which the density of states are at least one order of magnitude lower than those of the valence band. The result of Excitation II is like that of supra band gap excitation by absorbing a frequency doubled photon (200 nm), generating hot charge carriers to produce desorbing $^{\bullet}$OH radicals.

Similar to OH_t^-s, OH_b^- ions on TiO_2 are also predicted to capture holes [49,50], indicating that bridging hydroxyl radicals were likely also produced in our experiments. However, bidentate adsorption of the bridging hydroxyls (terminal hydroxyls bind monodentately) to the substrate likely prevented their desorption, which was consistent with the findings from the STM [19] and TPD [20] studies, where no change in the bridging hydroxyls on UV-illuminated TiO_2(110) was detected. Without desorption, bridg-

ing hydroxyl radicals would recombine with photogenerated electrons and decay back to hydroxyl anions on an ultrafast timescale. The reactivity of the photocatalyzed oxidation of hydroxyl anions was very low [24]. TD-2PPE could not detect the tiny transient electronic structure changes because of its limited sensitivity. The quantitative analysis is included in Supporting information. Therefore, no changes were detected at the H_2O/*r*-TiO_2 surface where the bridging hydroxyl anions existed.

Specifically, the easier desorption of terminal hydroxyl radicals led to the cumulative reduction of the substrate, while the more difficult desorption of the bridging hydroxyl radicals resulted in a reversible reaction. An electronic structure change from the cumulative reduction of the TiO_2 substrate was detectable by TD-2PPE. However, the tiny transient electronic structure change in a low activity reversible reaction was beyond the detection limit of conventional surface science techniques.

It has been reasoned that the terminal hydroxyl anions on TiO_2 cannot be oxidized because the positively charged Ti ions prevent holes from approaching the hydroxyl groups on top of the Ti ions, and the surface •OH radicals can only be generated at the bridging sites [18]. However, photocatalyzed oxidation reactions at the Ti_{5c} sites of TiO_2(110), such as the splitting of water, the conversion of methoxy anions into formaldehyde and the desorption of O_2, have been frequently reported [19–21,51–53]. Photocatalyzed oxidation of the OH_t^- ions on TiO_2(110) was observed in our study.

Based on these results, the assumption that Ti_{5c} ions repel holes is unreasonable. If the Ti_{5c} ions repelled holes, the Ti_{6c} ions under the bridging oxygen should also repel hole since they are also positively charged. The oxygen atoms of adsorbing OH_t^-s on TiO_2 are negatively charged [50]; thus, they can attract holes. In principle, most negatively charged oxygen species in TiO_2, for example, bulk oxygen atoms, terminal hydroxyls, terminal oxygen atoms, bridging oxygen atoms and bridging hydroxyls, can trap holes, and these have been predicted [49,50] and even experimentally detected [54–59]. Based on the site-specific photocatalyzed oxidation of the surface hydroxyls, the results from this surface science study indicates that the Ti_{5c} sites of TiO_2, which have been excluded from mechanistic studies of the photocatalyzed OER in solution [11,12], may actually provide a contribution to this oxidation [24,60].

The adsorption structure is the starting point for discussing surface chemistry. Our study confirmed that dissociative water, *i.e.*, terminal hydroxyls, are the active species in the photocatalyzed oxidation of water on TiO_2. Controversy regarding this issue in previous surface science studies [19,21] can now be rationalized by the coverage and external stimulus-dependent adsorption state of water on this surface.

The adsorption of water at Ti_{5c} of TiO_2(110) is sensitive to the surface structure, defects, impurities, coverages, temperature and the detection itself [26,27,32,35,61–63]. We focus on the liquid nitrogen temperature region at which our experiments were carried out. In this temperature range, molecular adsorption is generally preferred at monolayer coverages due to the formation of hydrogen bond networks [27,64]. At lower coverages, for example, below 0.05 ML, STM provides atomic resolved imaging of water adsorption. However, the relatively high voltages applied to bulk metal oxides can disturb the intrinsic adsorption. At a bias voltage of 1.2–1.6 V, the molecular adsorption of water at the Ti_{5c} sites of TiO_2(110) is likely preferred [62]. Another study using a bias voltage below 0.60 V showed that the dissociative adsorption was favored, producing terminal and bridging hydroxyl anions [63]. Core-level spectroscopy studies indicated mixed molecular and dissociative adsorption of water on TiO_2(110) at coverages below 0.4 ML [35].

In reference [19], the H_2O coverage was <0.05 ML, and dissociative adsorption was favored [63], so the photocatalyzed oxidation reaction was detected under UV light illumination. In reference [20,21], H_2O coverage was in the 0.10–1.00 ML range. Mixed adsorption occurred in the lower coverage region (<0.4 ML), and molecular adsorption dominated at higher coverages (>0.4 ML) [35]. Because the adsorption energy difference between the molecular and dissociative adsorption of H_2O on TiO_2(110) is small (several tens of meV) and the thermal activation barrier is in the 100-400 meV region [32,35,36,62,63,65–67], conversion between these two adsorption states in the presence of an external stimulus is possible. Femtosecond/picosecond lasers were used in reference [20,21]. Local heating by absorbing ultrashort pulses could provide energy for the molecular-to-dissociative water conversion. In addition, the peak electric field of the laser arriving at the surface was on the order of 10^{7-8} V/m, which was close to the electric field in the STM experiments. The electric field between the STM tip and the substrate was reported to cause a reduction in the thermal activation barrier of the reactions [63,68]. The high peak electric field potentially work together with local heating to affect the adsorption of water on TiO_2(110), resulting in the generation of terminal hydroxyl anions. Photothermal heating is dependent on the optical absorption [69]; this can lead to the wavelength-dependent generation of terminal hydroxyl anions and finally the wavelength-dependent photocatalyzed oxidation of water on TiO_2(110) [21].

The reason for inferred generation of gaseous •OH radicals from H_2O/TiO_2(110) under the irradiation of 355 nm and 400 nm light and the independence of the quantum yield on photon energy based on STM measurements [19], however, is not immediately clear. Maybe there is some possibility to produced gaseous •OH radicals under near band gap excitation. Because of the single molecule sensitivity, STM can detect it. But the negligible change is below the detection limit of other techniques such as TOF-MS and 2PPE. The extremely low quantum yield and the limited statistic sample may result in large error, leading to the independence of the quantum yield on photon energy.

•OH radicals are strong oxidative reagents in photocatalytic water purification and pollutant decomposition [70]. The production of •OH radicals in the gas phase [71–73] and solution bulk [54,55,74] from UV-illuminated TiO_2 has long been reported. The proposed mechanisms for •OH radical generation include direct oxidation of surface hydroxyl anions [25], reaction of water with trapped holes at bridging sites [74], reduction of H_2O_2 or O_2 [75] and photolysis of H_2O_2 and H_2O [71,76]. The current and previous studies [20,21] indicate that photocatalyzed oxidation of OH_t^-s on TiO_2 may provide a method for producing free •OH radicals.

Although desorption of •OH radicals from the photocatalyzed oxidation of OH_t^-s on TiO_2(110) has been detected [20,21], we cannot exclude the possibility of the generation of adsorbed •OH radicals at the terminal and bridging sites which have been theoretically predicted [49,50] and experimentally detected before [59]. Unfortunately, STM, TD-2PPE and TOF-MS cannot measure the surface radicals. Consequently, the transient surface species are missing from the analysis. However, X-ray free electron laser-based time-resolved X-ray spectroscopy can be used to monitor the transient low-concentration species [77].

Adsorption energy affects the release of •OH radicals from the surface. The OH_t^- and OH_b^- ions adsorb monodentately and bidentately at the Ti sites of TiO_2, respectively. Generally, bidentate adsorption is stronger than monodentate adsorption. The bonding configuration of the OH_t^- and OH_b^- ions to the Ti sites of TiO_2(110) potentially result in differences in the desorption of the terminal and bridging •OH radicals. The easier release of •OH radicals from anatase TiO_2 than from rutile TiO_2 is suggested to be responsible for the superior photocatalytic activity of the former [78].

OER in the photocatalyzed overall water splitting requires the coupling of two oxygen containing radicals to form O–O bond. Previous work [11,12] suggests the involvement of bridging oxygen

in O–O bond formation and excludes terminal hydroxyls by thinking that terminal hydroxyl anions on TiO_2 cannot be photocatalytically oxidized because of the level mismatch. This viewpoint, however, has been proven to be invalid by our results in the current work. So far, no consensus on the formation of O–O bond, *i.e.*, the origin of the oxygen atoms (O_b-O_b, O_t-O_t or O_b-O_t), has been reached. Theoretical calculations suggest that both O_t-O_t and O_b-O_t are possible [24,60,79]. Future direct site-specific measurements using STM are needed.

The HOMO of water and the hydroxyl groups on the TiO_2 surface are much lower than the substrate VBM (Fig. 2) [13,16,80]. The oxidization of these surface species by interfacial transfer of thermalized holes is conventionally considered to be unfavorable [13,14,16]. The $CH_3OH/TiO_2(110)$ system has a similar interfacial electronic structure to that of $H_2O/TiO_2(110)$, and the HOMOs of both CH_3OH_ts and $CH_3O_t^-$s are far below, and $eU^o_{CH_3O^-/CH_3O\bullet}$/$eU^o_{CH_3OH/CH_3OH^+}$ is located higher/lower than the VBM of TiO_2; however, in the $CH_3OH/TiO_2(110)$ system, the photocatalyzed oxidation of $CH_3O_t^-$s has been detected under near band gap excitation ($h\nu = 3.06$ eV) and CH_3OH_ts show no photoactivity [51].

Notably, Gibbs free energy ΔG is the criterion for determining whether a reaction can occur spontaneously, which is defined as the energy difference between the initial and final states. The reagent/substrate system and a complete free hole/electron can be regarded as the initial state of the reaction, which is obviously not the final state after capturing a hole/electron. The eU^o is the level at which the hole/electron is stabilized (Fig. 2), represents the final state of the reaction. Therefore, the eU^o rather than the HOMO/lowest unoccupied molecular orbital (LUMO) of the reagent should be taken to judge whether the reaction can thermodynamically occur [49,51]. According to reference [13], $eU^o_{OH^-/\bullet OH}$/$eU^o_{H_2O/H_2O^+}$ lies above/below the TiO_2 VBM (Fig. 2), indicating that the transfer of thermalized holes to OH_t^-/H_2O_t is thermodynamically favorable/unfavorable. The wavelength dependent production of gaseous $^\bullet$OH radicals [21] likely comes from the photon energy dependent desorption of surface $^\bullet OH_t$ radicals which adsorb tightly on TiO_2 [23].

In summary, the photocatalytic chemistry of water on *o*-$TiO_2(110)$ and *r*-$TiO_2(110)$ initiated by 400 nm light illumination was investigated and compared to understand the mechanism of water oxidation. Through the combined TD-2PPE, XPS and TPD measurements, we suggested the photocatalyzed oxidation of water on $TiO_2(110)$ and identified the terminal Ti_{5c} sites and the OH_t^- ions as the active sites and active species, respectively. Based on our results, the terminal Ti_{5c} sites and the oxidation of the hydroxyl groups on top of them on TiO_2, which were previously disregarded in solution, needed to be considered in the exploration of the mechanism of the photocatalyzed OER.

Declaration of competing interest

The authors declare that they have no known competing financial interests or personal relationships that could have appeared to influence the work reported in this paper.

CRediT authorship contribution statement

Zhiqiang Wang: Writing – review & editing, Writing – original draft, Investigation, Funding acquisition. **Yajie Gao:** Investigation, Data curation. **Tianjun Wang:** Formal analysis, Data curation. **Wei Chen:** Formal analysis, Data curation. **Zefeng Ren:** Investigation, Formal analysis, Data curation. **Xueming Yang:** Supervision, Project administration, Funding acquisition. **Chuanyao Zhou:** Writing – review & editing, Writing – original draft, Supervision, Resources, Project administration, Funding acquisition, Conceptualization.

Acknowledgments

This work was supported by the National Key Research and Development Program of China (No. 2021YFA1500601), the National Natural Science Foundation of China (Nos. 22322306 and 22288201), the Chinese Academy of Sciences (Nos. YSBR-007, XDB0970000), the Key Research Project of Shaanxi Provincial Science and Technology Department (No. 2023-YBNY-158), the Xi'an Science and Technology Project (No. 22NYYF016), and the 111 Project. We thank Sen Feng from Dalian Institute of Chemical Physics for his assistance in the acquisition of XPS and TPD data.

Supplementary materials

Supplementary material associated with this article can be found, in the online version, at doi:10.1016/j.cclet.2024.110602.

References

[1] A. Fujishima, K. Honda, Nature 238 (1972) 37–38.
[2] X.B. Chen, S.H. Shen, L.J. Guo, et al., Chem. Rev. 110 (2010) 6503–6570.
[3] A.L. Linsebigler, G.Q. Lu, J.T. Yates, Chem. Rev. 95 (1995) 735–758.
[4] E.D. Fakhrutdinova, O.A. Reutova, T.A. Bugrova, et al., Trans. Tianjin Univ. 30 (2024) 198–209.
[5] W. Navarra, I. Ritacco, O. Sacco, et al., J. Phys. Chem. C 126 (2022) 7000–7011.
[6] S. Du, J. Lian, F. Zhang, Trans. Tianjin Univ. 28 (2022) 33–52.
[7] M. Zhou, H.F. Wang, Chin. Chem. Lett. 33 (2022) 4705–4709.
[8] Y. Jiang, Y. Qin, T. Yu, et al., Chin. Chem. Lett. 32 (2021) 1823–1826.
[9] Z. Wu, F. Xiong, Z. Wang, et al., Chin. Chem. Lett. 29 (2018) 752–756.
[10] Y. Ma, X. Wang, Y. Jia, et al., Chem. Rev. 114 (2014) 9987–10043.
[11] R. Nakamura, Y. Nakato, Solid State Phenomena 162 (2010) 1–27.
[12] P. Salvador, Prog. Surf. Sci. 86 (2011) 41–58.
[13] A. Imanishi, T. Okamura, N. Ohashi, et al., J. Am. Chem. Soc. 129 (2007) 11569–11578.
[14] R. Nakamura, Y. Nakato, J. Am. Chem. Soc. 126 (2004) 1290–1298.
[15] Q. Guo, C. Zhou, Z. Ma, et al., Chem. Soc. Rev. 45 (2016) 3701–3730.
[16] P. Salvador, J. Phys. Chem. C 111 (2007) 17038–17043.
[17] Y. Nosaka, A. Nosaka, ACS Energy Lett. 1 (2016) 356–359.
[18] Y. Nosaka, A.Y. Nosaka, Chem. Rev. 117 (2017) 11302–11336.
[19] S. Tan, H. Feng, Y. Ji, et al., J. Am. Chem. Soc. 134 (2012) 9978–9985.
[20] W. Yang, D. Wei, X. Jin, et al., J. Phys. Chem. Lett. 7 (2016) 603–608.
[21] C. Xu, F. Xu, X. Chen, et al., J. Phys. Chem. Lett. 12 (2021) 1066–1072.
[22] Z. Geng, X. Chen, W. Yang, et al., J. Phys. Chem. C 120 (2016) 26807–26813.
[23] A. Migani, L. Blancafort, J. Am. Chem. Soc. 139 (2017) 11845–11856.
[24] D. Wang, T. Sheng, J. Chen, et al., Nat. Catal. 1 (2018) 291–299.
[25] U. Diebold, Surf. Sci. Rep. 48 (2003) 53–229.
[26] L.E. Walle, A. Borg, P. Uvdal, et al., Phys. Rev. B 80 (2009) 235436.
[27] M.A. Henderson, Surf. Sci. 355 (1996) 151–166.
[28] M.A. Henderson, W.S. Epling, C.H.F. Peden, et al., J. Phys. Chem. B 107 (2003) 534–545.
[29] R.T. Zehr, M.A. Henderson, Surf. Sci. 602 (2008) 1507–1516.
[30] M. Li, W. Hebenstreit, L. Gross, et al., Surf. Sci. 437 (1999) 173–190.
[31] E. Lira, J.O. Hansen, P. Huo, et al., Surf. Sci. 604 (2010) 1945–1960.
[32] Y. Du, N.A. Deskins, Z. Zhang, et al., Phys. Rev. Lett. 102 (2009) 096102.
[33] W.S. Epling, C.H.F. Peden, M.A. Henderson, et al., Surf. Sci. 413 (1998) 333–343.
[34] Z. Zhang, Y. Du, N.G. Petrik, et al., J. Phys. Chem. C 113 (2009) 1908–1916.
[35] C. Kamal, N. Stenberg, L.E. Walle, et al., Phys. Rev. Lett. 126 (2021) 016102.
[36] M. Amft, L.E. Walle, D. Ragazzon, et al., J. Phys. Chem. C 117 (2013) 17078–17083.
[37] C.Y. Zhou, Z.B. Ma, Z.F. Ren, et al., Energ. Environ. Sci. 5 (2012) 6833–6844.
[38] K. Onda, B. Li, H. Petek, Phys. Rev. B 70 (2004) 045415.
[39] K. Onda, B. Li, J. Zhao, et al., Science 308 (2005) 1154–1158.
[40] C.M. Yim, C.L. Pang, G. Thornton, Phys. Rev. Lett. 104 (2010) 036806.
[41] X.C. Mao, X.F. Lang, Z.Q. Wang, et al., J. Phys. Chem. Lett. 4 (2013) 3839–3844.
[42] Z. Wang, B. Wen, Q. Hao, et al., J. Am. Chem. Soc. 137 (2015) 9146–9152.
[43] J. Li, T. Wang, S. Xia, et al., JACS Au 4 (2024) 491–501.
[44] V. Henrich, G. Dresselhaus, H. Zeiger, Phys. Rev. Lett. 36 (1976) 1335–1339.
[45] S. Wendt, P.T. Sprunger, E. Lira, et al., Science 320 (2008) 1755–1759.
[46] T.L. Thompson, J.T. Yates Jr., J. Phys. Chem. B 109 (2005) 18230–18236.
[47] C.B. Xu, W.S. Yang, Q. Guo, et al., Chin. J. Chem. Phys. 26 (2013) 646–650.
[48] Y. Du, N.A. Deskins, Z. Zhang, et al., J. Phys. Chem. C 114 (2010) 17080–17084.
[49] J. Cheng, J. VandeVondele, M. Sprik, J. Phys. Chem. C 118 (2014) 5437–5444.
[50] D. Wang, H. Wang, P. Hu, Phys. Chem. Chem. Phys. 17 (2015) 1549–1555.
[51] S. Dong, J. Hu, S. Xia, et al., ACS Catal. 11 (2021) 2620–2630.
[52] M. Shen, M.A. Henderson, J. Phys. Chem. Lett. 2 (2011) 2707–2710.
[53] Z.T. Wang, N. Aaron Deskins, I. Lyubinetsky, J. Phys. Chem. Lett. 3 (2012) 102–106.

[54] C.D. Jaeger, A.J. Bard, J. Phys. Chem. 83 (1979) 3146–3152.
[55] M. Anpo, T. Shima, Y. Kubokawa, Chem. Lett. 14 (1985) 1799–1802.
[56] R.F. Howe, M. Gratzel, J. Phys. Chem. 91 (1987) 3906–3909.
[57] O.I. Micic, Y. Zhang, K.R. Cromack, et al., J. Phys. Chem. 97 (1993) 7277–7283.
[58] P.F. Schwarz, N.J. Turro, S.H. Bossmann, et al., J. Phys. Chem. B 101 (1997) 7127–7134.
[59] Y. Nosaka, S. Komori, K. Yawata, et al., Phys. Chem. Chem. Phys. 5 (2003) 4731–4735.
[60] H. Zhou, X. Zhang, J. Zhang, et al., J. Mater. Chem. A 9 (2021) 7650–7655.
[61] I.M. Brookes, C.A. Muryn, G. Thornton, Phys. Rev. Lett. 87 (2001) 266103–266106.
[62] Z.T. Wang, Y.G. Wang, R. Mu, et al., Proc. Natl. Acad. Sci. U. S. A. 114 (2017) 1801–1805.
[63] S. Tan, H. Feng, Q. Zheng, et al., J. Am. Chem. Soc. 142 (2020) 826–834.
[64] K. Sebbari, C. Domain, J. Roques, et al., Surf. Sci. 605 (2011) 1275–1280.
[65] S. Wendt, J. Matthiesen, R. Schaub, et al., Phys. Rev. Lett. 96 (2006) 066107.
[66] P.J.D. Lindan, C.J. Zhang, Phys. Rev. B 72 (2005) 075439.
[67] L.A. Harris, A.A. Quong, Phys. Rev. Lett. 93 (2004) 086105.
[68] X. Meng, J. Guo, J. Peng, et al., Nat. Phys. 11 (2015) 235–239.
[69] R. Feng, A. Liu, S. Liu, et al., J. Phys. Chem. C 119 (2015) 9798–9804.
[70] A. Mills, R.H. Davies, D. Worsley, Chem. Soc. Rev. 22 (1993) 417–425.
[71] Y. Murakami, E. Kenji, A.Y. Nosaka, et al., J. Phys. Chem. B 110 (2006) 16808–16811.
[72] Y. Murakami, K. Endo, I. Ohta, et al., J. Phys. Chem. C 111 (2007) 11339–11346.
[73] J. Thiebaud, F. Thévenet, C. Fittschen, J. Phys. Chem. C 114 (2010) 3082–3088.
[74] J. Zhang, Y. Nosaka, J. Phys. Chem. C 118 (2014) 10824–10832.
[75] M.R. Hoffmann, S.T. Martin, W.Y. Choi, et al., Chem. Rev. 95 (1995) 69–96.
[76] B.H.J. Bielski, D.E. Cabelli, R.L. Arudi, et al., J. Phys. Chem. Ref. Data 14 (1985) 1041–1100.
[77] Z.H. Loh, G. Doumy, C. Arnold, et al., Science 367 (2020) 179–182.
[78] W. Kim, T. Tachikawa, G.H. Moon, et al., Angew. Chem. 126 (2014) 14260–14265.
[79] G.H. Ren, M. Zhou, P.J. Hu, et al., Nat. Commun. 15 (2024) 2346.
[80] R.L. Kurtz, R. Stock-Bauer, T.E. Msdey, et al., Surf. Sci. 218 (1989) 178–200.